Sub Topic: Novel Combustion Techniques

13th U.S. National Combustion Meeting
Organized by the Central States Section of the Combustion Institute
March 19-22, 2023
College Station, Texas

OpenFOAM solver for volume-averaged modeling of porous media burners

Aniruddha Saha[*1] *and Sadaf Sobhani*[1]

[1]*Department of Mechanical and Aerospace Engineering, Cornell University, NY, USA*
[*]*Corresponding Author:* as2742@cornell.edu

Abstract: A new OpenFOAM solver for porous media combustion is presented based on a volume-averaged formulation, assuming thermal non-equilibrium in the gas-solid system. The non-catalytic combustion dynamics of methane/air flames are simulated, and results for flame temperature, emissions and stability are shown.
Keywords: Porous media combustion, OpenFOAM, Computation

1. Introduction

Combustion in porous media burners (PMBs) enable enhanced flame stabilization and reduced emissions as compared to conventional burners. These properties result from the recirculation of heat generated from combustion by conduction and radiation through the solid matrix [1, 2]. The balance between heat recirculated through the matrix, generated at the reaction zone and lost via radiation to the surroundings determines flame stabilization and emissions behavior [3–6]. These properties are also highly dependent on the geometry [7, 8] of the porous material [1, 9, 10]. Reducing unburnt hydrocarbons, CO and NO_x emissions [11, 12] as well as increasing flame stability are some of the key aims of PMB research and development.

Along with numerous experimental studies [5, 13–16], pore-scale and volume-averaged simulations have been applied extensively to study PMB behavior. Pore scale simulations have been performed to give insight into the flow, chemical, and thermal transport properties at the 'micro' scale, i.e., within the void space [17, 18], but are generally too computationally expensive to perform in large-scale domains. Such simulations capture the effect of pore geometry on the combustion process. Volume-averaged methods, on the other hand, are less computationally expensive, but describe only macroscopic characteristics of PMB behavior based on closure models for the subgrid scale dynamics [19–21]. PMB operation with CH_4/air premixed flames of various equivalence ratios has been the focus of numerous studies [20, 22, 23]. Furthermore, most studies investigate the two-zone step burner, in which the flame stabilizes at the interface of two zones, i.e., the upstream and downstream porous sections [24, 25].

In this work, a new volume-averaged finite-volume solver is presented for volume-averaged modeling of porous media combustion. This solver is developed using OpenFOAM, an open-source software framework. This study focuses on CH_4/air flames in two zone PMBs to facilitate comparisons with literature. Gas temperature, NO and CO profiles for a 1D PMB are presented here, with future work focusing on 2D and 3D simulations.

2. Computational Methodology

A volume-averaged approach is adopted to study the combustion of the gaseous mixture and the thermodynamic coupling of the gas-solid system. The thermophysical properties such as the effective thermal conductivity $\lambda_{s,\text{eff}}$ and the volumetric heat transfer coefficient h_v are functions of the porosity distribution. The simulations are based on the governing equations of porous media combustion [26] accompanied by the ideal gas equation of state. Heat conduction occurs in both the solid and gas phases. We consider the phase-averaged Darcy velocity $\mathbf{U} = \phi\mathbf{u}$, where ϕ is the porosity and $\mathbf{u}$ is the actual velocity[27]. $\bar{T}$ and $\bar{T}_\text{s}$ represent the averaged gas and solid temperatures, respectively. The effective thermal conductivity [28] of the solid can be defined as $\lambda_{s,\text{eff}} = \phi\lambda_g + (1-\phi)\lambda_s + d_m\sigma e\bar{T}_s^3$. The governing equations are:

$$\bar{\nabla}\cdot\mathbf{U} = 0 \tag{1a}$$

$$\rho\left[\frac{\partial}{\partial t}(\mathbf{U}) + \bar{\nabla}\cdot\left((1+c)\mathbf{U}\mathbf{U}/\phi\right)\right] = -\bar{\nabla}(\phi P) + \rho\bar{\nabla}\cdot[(\nu+\varepsilon)\bar{\nabla}(\mathbf{U})] \tag{1b}$$

$$\rho c_\text{pg}\frac{\partial(\phi\bar{T})}{\partial t} + \rho c_\text{pg}\bar{\nabla}\cdot(\mathbf{U}\bar{T}) = \lambda_g\bar{\nabla}\cdot(\phi\nabla\bar{T}) + h_v(\bar{T}_\text{s} - \bar{T}) \tag{1c}$$

$$\rho_\text{s}c_\text{ps}(1-\phi)\frac{\partial\bar{T}_\text{s}}{\partial t} = \bar{\nabla}\left(\lambda_{s,\text{eff}}\bar{\nabla}\bar{T}_\text{s}\right) - h_v(\bar{T}_\text{s} - \bar{T}) \tag{1d}$$

$$\phi\rho\frac{\partial Y_i}{\partial t} + \phi\rho\mathbf{U}\cdot\nabla Y_i = \rho\nabla\cdot(\phi D_{im}\nabla Y_i) + \phi\dot{\omega} \tag{1e}$$

where $\phi\dot{\omega}$ is the source term of the reaction, $D_{im} = \frac{1-X_i}{\sum_{\substack{j=1\\ j\neq i}}^{N}\frac{X_j}{D_{ij}}}$ is the species-mixture diffusion coefficients, and $c_\text{pg} = \sum_{i=1}^{N} Y_i c_{pg,i}$ is the specific heat capacity of the gas-mixture. The PMB is modeled as a two-zone step burner, wherein the discrete properties of each zone are approximated as a smoothly transitioning hyperbolic tangent profile. The boundary conditions are fixed equivalence ratio and temperature at the inlet, and zero gradient solid temperature, radiative blackbody to 298K heat flux, and zero gradient species concentration at the outlet.

The governing equations are solved using the C++ based finite volume simulation toolbox OpenFOAM for its object-oriented framework and thermophysical models. The momentum equation is solved using the PIMPLE algorithm. The reaction is calculated through the time-evolution of the concentration of the species, using GRI 3.0 mechanism. The flow through porous media is presented using volume-averaged methods where a single modified momentum equation is solved for the fluid-solid matrix.

3. Results and Discussion

A parametric study, in which the properties of the two sections are varied independently, is presented. The results confirm that matrix properties significantly affect the stable operating range among other properties. In addition, the upstream section acts primarily as a flashback arrestor and for the widest operating range, it should have a low conductivity and high volumetric heat transfer coefficient. The downstream section acts primarily to recirculate heat through the matrix; it should

have a high conductivity and low volumetric heat transfer coefficient. A stable flame is identified as a stationary solution of the set of governing equations.

First, to validate the computations, results are compared to that of Barra et al. [23]. Here, equivalence ratio $\phi = 0.65$ and the two sections of the burner have porosities of 0.835 and 0.87. Results indicate good agreement in the temperature profiles, with a peak temperature difference of 40 K, as shown in Fig. 1. The difference is attributed to the different numerical approach and the chemistry modelling, since Barra et al. use GRI 1.2 mechanism and GRI 3.0 is used in this work.

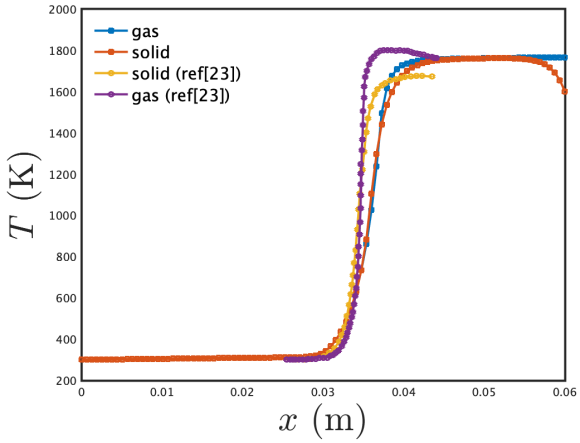

Figure 1: Temperature profile comparison for solid and gas phases

Next, the influence of geometry profiles, as shown in Fig. 2, on flame behavior was investigated. The porosities of the left and right section are kept at 0.835 and 0.87 respectively. This smoothness in ε is also reflected in pore diameter d_m. This design is achieved mathematically using $\varepsilon \propto \tanh[B(x-x_0)]$, with $B = 6, 8, 10$ for burners 1,2 and 3 respectively.The different burners that have been described are used to understand the effect of a smooth variation of material properties under identical inlet velocities of 0.4 m/s and an equivalence ratio of 0.7. As shown in Fig. 3(a), the stable flame position shifts upstream as we use a steeper variation. Although there is a decrease in NO emissions for a steeper profile in Fig. 3(b), CO exit emissions remain mostly unchanged. It is interesting to observe that without significant changes in peak temperatures, the NO emissions decrease with steeper profiles.

Next, the effect of equivalence ratio on the gas temperature distribution and NO, CO distribution for a stable flame are investigated and results shown in Fig. 4 and 5. The inlet velocities are considered to be same at 0.25 m/s in Fig. 4 and the maximum stable velocities of 0.25, 0.37 and 0.48 m/s are considered for equivalence ratios of 0.7, 0.8 and 0.9 respectively in Fig. 5. The flame is anchored near the interface for all stable conditions. The generation of NO and CO is dependent on the temperature of the reaction. The emissions increase with the equivalence ratio as seen in Fig. 4(b) and (c) which is also observed in Ref.[29] and the distribution shifts downstream as the velocity increases as seen in Fig. 5(b) and (c). For lower velocities, the gaseous mixture is exposed to higher temperatures for longer times, therefore NO production is increased. As the equivalence ratio increases, the amount of air relative to the hydrocarbon decreases, leading to higher CO emissions.

Next, the sensitivity of the volumetric heat transfer coefficient on flame behavior is investi-

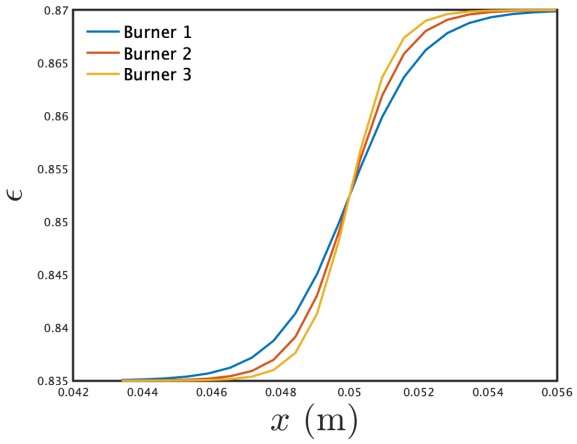

Figure 2: The different burners having different smoothness of transition of properties.

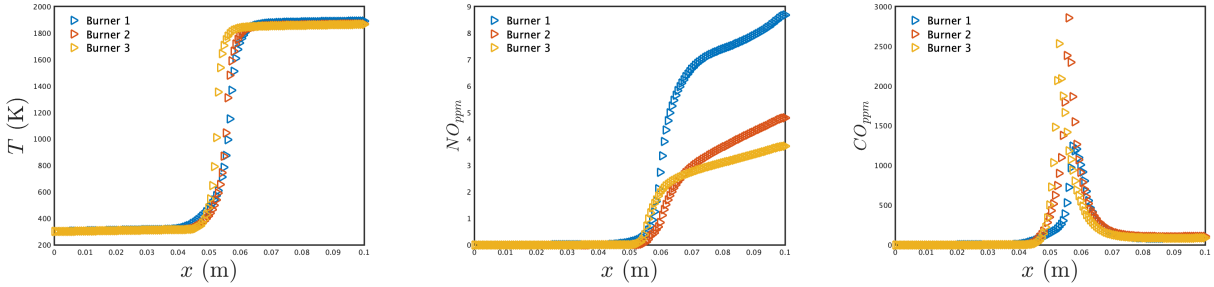

Figure 3: Gas temperature profiles and distribution of NO and CO for different burners.

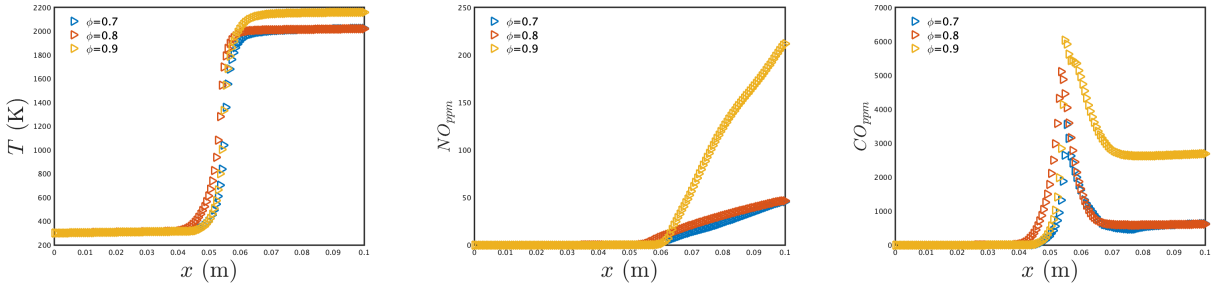

Figure 4: Gas temperature profiles and distribution of NO and CO for different equivalence ratios for same inlet velocities.

gated. Using equivalent porosity and pore diameter distributions, two different models for h_v are studied from [30] and [21]. Additionally, a third burner model with smoothly graded ($B = 10$) thermal conductivity from 1 W/mK to 0.2 W/mK was investigated. The results are shown in Fig. 6 where it is observed tthat a new stable flame position is attained, while keeping the temperature and the emissions same. This shows the independent optimization of the operational variables. Predicted exit temperature and emissions are highly sensitive to the thermal properties of the burner. Therefore, suitable constitutive relations in volume-averaged methods are significant for determin-

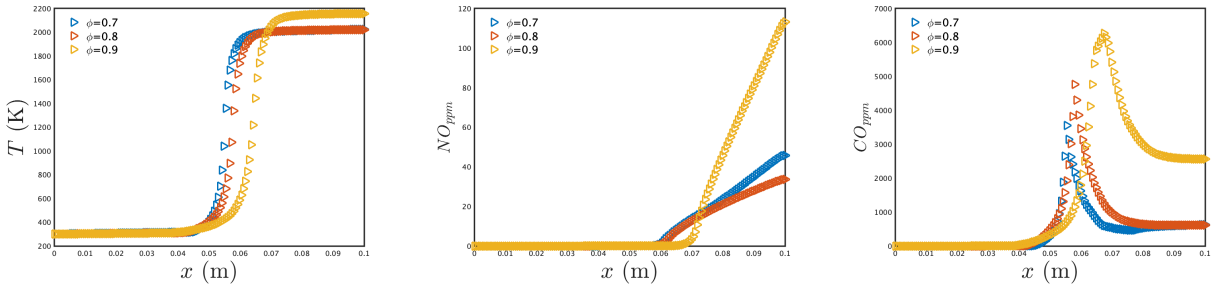

Figure 5: Gas temperature profiles and distribution of NO and CO for different equivalence ratios with maximum stable inlet velocities.

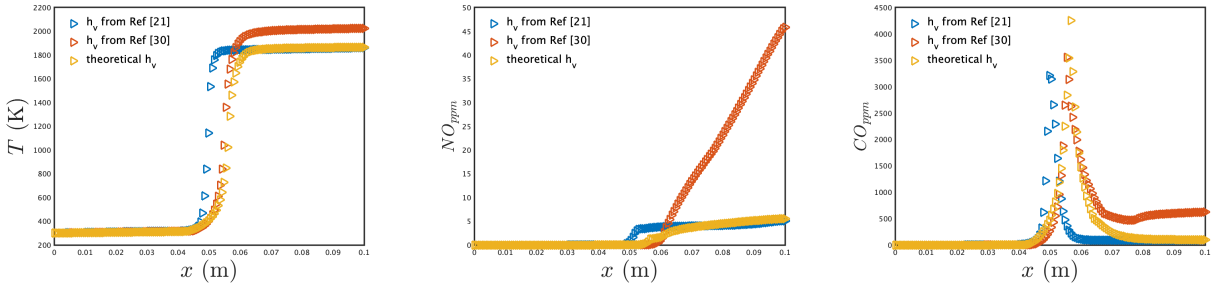

Figure 6: Gas temperature profiles and distribution of NO and CO for different heat transfer coefficients .

ing model fidelity. Furthermore, different constitutive relations can be used to describe the heat transfer properties of various porous materials. This opens up new avenues for materials design for regulating emissions and flame stability, by using additive manufacturing to architect specific porous structures for PMBs [31]. Determining proper thermal constitutive models and optimized geometric profiles for burner performance are the aims of ongoing work.

4. Conclusion

In this work, a new solver based on open-source CFD toolbox OpenFOAM is presented for simulating porous media combustion. The chemical kinetics are modeled using the GRI 3.0 mechanism. Results for various 1D step two-zone porous media burners are presented. Since the solver is fully three-dimensional, future work will focus on expanding these results to higher dimensions and leveraging insights about the porous geometry-flame behavior relationship to design advanced burners using additive manufacturing.

References

[1] W. M. Mathis and J. L. Ellzey, Flame stabilization, operating range, and emissions for a methane/air porous burner, Combustion Science and Technology 175 (2003) 825–839.

[2] Y. Yoshio, S. Kiyoshi, and E. Ryozo, Analytical study of the structure of radiation controlled flame, International Journal of Heat and Mass Transfer 31 (1988) 311–319.

[3] A. J. Barra and J. L. Ellzey, Heat recirculation and heat transfer in porous burners, Combustion and flame 137 (2004) 230–241.

[4] A. J. Barra, G. Diepvens, J. L. Ellzey, and M. R. Henneke, Numerical study of the effects of material properties on flame stabilization in a porous burner, Combustion and Flame 134 (2003) 369–379.

[5] O. Pickenacker and D. Trimis, Experimental study of a staged methane/air burner based on combustion in a porous inert medium, Journal of porous media 4 (2001).

[6] J. F. Liu and W. H. Hsieh, Experimental investigation of combustion in porous heating burners, combustion and Flame 138 (2004) 295–303.

[7] S. A. Shakiba, R. Ebrahimi, M. Shams, and Z. Yazdanfar, Effects of foam structure and material on the performance of premixed porous ceramic burner, Proceedings of the Institution of Mechanical Engineers, Part A: Journal of Power and Energy 229 (2015) 176–191.

[8] D. Trimis and F. Durst, Combustion in a porous medium-advances and applications, Combustion science and technology 121 (1996) 153–168.

[9] C. Tierney, S. Wood, A. T. Harris, and D. F. Fletcher, Computational Fluid Dynamics modelling of ultra-lean porous burners, Progress in Computational Fluid Dynamics 10 (2010) 352–365.

[10] C. H. Smith, D. I. Pineda, and J. L. Ellzey, Syngas production from burner-stabilized methane/air flames: The effect of preheated reactants, Combustion and flame 160 (2013) 557–564.

[11] P. Bouma and L. De Goey, Premixed combustion on ceramic foam burners, Combustion and Flame 119 (1999) 133–143.

[12] C. Keramiotis, B. Stelzner, D. Trimis, and M. Founti, Porous burners for low emission combustion: An experimental investigation, Energy 45 (2012) 213–219.

[13] S. Sobhani, B. Haley, D. Bartz, J. Dunnmon, J. Sullivan, and M. Ihme, Investigation of lean combustion stability, pressure drop, and material durability in porous media burners, Turbo Expo: Power for Land, Sea, and Air (2017), V05CT17A001.

[14] J. Howell, M. Hall, and J. Ellzey, Combustion of hydrocarbon fuels within porous inert media, Progress in Energy and Combustion Science 22 (1996) 121–145.

[15] S. Sobhani, P. Muhunthan, E. Boigné, D. Mohaddes, and M. Ihme, Experimental feasibility of tailored porous media burners enabled via additive manufacturing, Proceedings of the Combustion Institute 38 (2021) 6713–6722.

[16] S. Sobhani, D. Mohaddes, E. Boigne, P. Muhunthan, and M. Ihme, Modulation of heat transfer for extended flame stabilization in porous media burners via topology gradation, Proceedings of the Combustion Institute 37 (2019) 5697–5704.

[17] P.-L. Billerot, L. Dufresne, R. Lemaire, and P. Seers, 3D CFD analysis of a diamond lattice-based porous burner, Energy 207 (2020) 118160.

[18] I. Yakovlev and S. Zambalov, Three-dimensional pore-scale numerical simulation of methane-air combustion in inert porous media under the conditions of upstream and downstream combustion wave propagation through the media, Combustion and Flame 209 (2019) 74–98.

[19] A. B. Caldeira and Ç. Susantez, A simplified numerical approach to hydrogen and hydrocarbon combustion in single and double-layer porous burners, International Journal of Hydrogen Energy 45 (2020) 35235–35245.

[20] S. M. Hashemi and S. A. Hashemi, Flame stability analysis of the premixed methane-air combustion in a two-layer porous media burner by numerical simulation, Fuel 202 (2017) 56–65.

[21] S. N. Hoda, S. A. G. Nassab, and J. J. Ebrahim, Three dimensional numerical simulation of combustion and heat transfer in porous radiant burners, international journal of thermal sciences 145 (2019) 106024.

[22] S. Sathe, M. Kulkarni, R. Peck, and T. Tong, An experimental and theoretical study of porous radiant burner performance, Symposium (International) on Combustion (1991), pp. 1011–1018.

[23] A. J. Barra, G. Diepvens, J. L. Ellzey, and M. R. Henneke, Numerical study of the effects of material properties on flame stabilization in a porous burner, Combustion and Flame 134 (2003) 369–379.

[24] H. Gao, Z. Qu, X. Feng, and W. Tao, Methane/air premixed combustion in a two-layer porous burner with different foam materials, Fuel 115 (2014) 154–161.

[25] H. Gao, Z. Qu, X. Feng, and W. Tao, Combustion of methane/air mixtures in a two-layer porous burner: A comparison of alumina foams, beads, and honeycombs, Experimental Thermal and Fluid Science 52 (2014) 215–220.

[26] M. Kaviany, Principles of heat transfer in porous media, Springer Science & Business Media, 2012.

[27] K. Vafai, Handbook of porous media, Crc Press, 2015.

[28] M. J. de Lemos, Numerical simulation of turbulent combustion in porous materials, International Communications in Heat and Mass Transfer 36 (2009) 996–1001.

[29] V. Bubnovich, L. Henriquez, and N. Gnesdilov, Numerical study of the effect of the diameter of alumina balls on flame stabilization in a porous-medium burner, Numerical Heat Transfer, Part A: Applications 52 (2007) 275–295.

[30] X. Fu, R. Viskanta, and J. Gore, Measurement and correlation of volumetric heat transfer coefficients of cellular ceramics, Experimental Thermal and Fluid Science 17 (1998) 285–293.

[31] S. Sobhani, S. Allan, P. Muhunthan, E. Boigne, and M. Ihme, Additive Manufacturing of Tailored Macroporous Ceramic Structures for High-Temperature Applications, Advanced Engineering Materials 22 (2020) 2000158.